Brazilian Journal of Physics (2020) 50:331–345
https://doi.org/10.1007/s13538-020-00737-y

SOCIEDADE BRASILEIRA DE FÍSICA

NUCLEAR PHYSICS

Systematic Calculation of Neutrino–Nucleus Cross Section Available for Astrophysical Applications

C. A. Barbero[1,2] · M. Cassiano dos Santos[3] · A. R. Samana[3]

Received: 14 October 2019 / Published online: 3 March 2020
© Sociedade Brasileira de Física 2020

Abstract

Assuming the universality of weak interactions, we have studied the weak processes such as β-decay and electron capture using the nuclear gross theory of beta decay (GTBD). We evaluate the $\beta^{\pm}$ and electron capture decay rates and the neutrino–nucleus cross sections as a function of the energy of the incident neutrino, for $E_\nu < 250$ MeV. The evaluation performed some years ago for the electron neutrino–nucleus reactions in the mass region $A < 70$ is extended to the heavy one $A < 220$ for a set of 965 nuclear species of astrophysical interest. The nuclei are separated according to its parity in even–even, even–odd, odd–odd, and odd–even nuclei, both for $\beta^{\pm}$-decay and electron capture. The obtained cross sections are interpolated by means of a fourth-degree polynomial function in E_ν. The coefficients in these polynomials are obtained and later fitted as a function of A and Z. The fitting procedure is described in detail paying special attention to the root mean square deviations in the adjustment. These polynomial functions provide a tool for the systematic evaluation of the cross sections needed in astrophysical processes like the r-process during the nucleosynthesis of supernovae.

Keywords β-decay · Electron capture · Neutrino–nucleus cross section · Gross theory of beta decay

1 Introduction

In recent years, the weak neutrino–nucleus interactions have been widely studied both experimentally and theoretically, since neutrino properties that are still under discussion can be inferred, such as their mass. Many experiments intended to find exotic neutrino properties, such as oscillations, use the ^{12}C nucleus in the scintillation detectors. Other nuclei such as ^{37}Cl, ^{16}O, ^{20}Ne, and ^{56}Fe [1–3] are used as detectors, and others such as ^{40}Ar and ^{208}Pb are neutrino targets in detectors such as ICARUS Collaboration [4], ArgoNeut Collaboration [5], and HALO Collaboration [6]. In several works, it has been shown that the nuclear structure calculations greatly affect the measurements and uncertainties of the properties studied [7]. In this way, neutrino-nucleus cross sections are so important to understand the exotic properties of neutrinos [8] as well as the stellar models are to understand the stellar collapse process. The physical quantity measurable is the average cross section, $\langle\sigma(T_\nu)\rangle$, which depends on the temperature of the incident neutrino, T_ν, and is calculated convolving the cross section for the reaction $\nu_e + (Z, A) \rightarrow (Z + 1, A) + e^-$, $\sigma_\nu(E_\nu)$, which depends on the energy of the incident neutrino, E_ν, with the theoretical thermal flux of neutrinos emitted in supernovae, $\Phi_\nu(E_\nu, T_\nu)$, i.e., [9]

$$\langle\sigma_\nu(T_\nu)\rangle = \int_{E_{\rm th}}^{\infty} \Phi_\nu(E_\nu, T_\nu)\sigma(E_\nu)dE_\nu, \quad (1)$$

where $E_{\rm th}$ is the reaction energy threshold, which is equal to the Q value for stable nuclei and zero for unstable cases. We have scarce experimental data of $\sigma(E_\nu)$ for the case of electron neutrino on the ground state of ^{12}C in the experiment LSND (liquid scintillator neutrino detector) [10–14]. Depending on the neutrino flux used, it will give us important information about some of the exotic properties of neutrinos, such as their mass. Within the standard model (SM), the neutrino mass is equal to zero for all neutrino flavors, but for physics beyond the SM, the mass is different from zero and even more, it would be different for each neutrino, depending on its flavor. The calculation of the

✉ C. A. Barbero
cab@fisica.unlp.edu.ar

1 Departamento de Física, Universidad Nacional de La Plata, C. C. 67, 1900 La Plata, Argentina

2 Instituto de Física La Plata, CONICET, 1900 La Plata, Argentina

3 Departamento de Ciencias Exatas e Tecnologicas, Universidade Estadual de Santa Cruz, Ilhéus, BA, Brazil

cross section depends strongly on the nuclear model used and the energy of the incident neutrino. Within the nuclear models describing interactions of neutrino with nucleus, we can mention (i) microscopic models like the RPA (random phase approximation), the QRPA (quasiparticle random phase approximation), and the SM; (ii) macroscopic models, such as the Fermi gas model, relativistic, and non-relativistic; (iii) semi-microscopic models where shell effects or pairing are included, such as the gross theory of beta decay (GTBD) [9].

In nuclear astrophysics, the processes involving strong, weak, and electromagnetic interactions are of fundamental importance. Within nuclear reactions, we have thermonuclear and scattering reactions. The thermonuclear reactions take place in the stars and include capture of nuclei and α particles, relevant for the stellar energy balance, and also to determine the relative abundance of the elements observed in nature. Scattering reactions occur at low temperature and low average densities and are produced by interactions of particles thermally accelerated up to a few tenths of MeV/nucleon with the stellar medium. The β-decay, as well as the electrons capture (EC) or positrons capture are fundamental in the scenario of stellar evolution (presupernova and supernova) and for nucleosynthesis (the r-process). The observed capture rates compete, under certain stellar conditions, with neutrino capture rates and, for example, can modify the trajectory of the r-process [15]. The neutrino capture rates are calculated using the neutrino–nucleus cross sections.

The literature describing calculations of neutrino–nucleus cross sections has varied since the early works of O'Connell, Donnelly, and Walecka in the 1970s [16]. For example, Borzov and collaborators [17] showed that, using the interaction of neutrino with ^{16}O, different calculations of nuclear structure can be used with different energies of the incident neutrino. As shown in Figure 1 from [17], the cross sections as a function of the energy for SM have a lower value than for the QRPA in the case of antineutrinos; but they have values greater, equal, and smaller in the case of neutrinos. For example, for electron neutrino (ν_e) energies above 50 MeV, the cross sections obtained within the SM and QRPA models have a similar behavior. As discussed in that reference, none of these models is recommended for neutrinos with energies $100 \leq E_{\nu_e} \leq 500$ MeV neither exceeding this limit. For $E_{\nu_e} \simeq 300$ MeV, the relativistic Fermi gas model give better results than the QRPA. For $E_{\nu_e} \sim 500$ MeV, the QRPA and the relativistic Fermi gas model give similar results. Otherwise, for the interaction of muon neutrino (ν_μ) with nuclei, the authors compared these two models for $E_{\nu_\mu} < 200$ MeV, noting that the QRPA is not a good model for $E_{\nu_\mu} \geq 200$ MeV. Our group has calculated neutrino–nucleus cross sections using both microscopic and macroscopic models: (i) for nuclei with $A \leq 70$ using the GTBD model [9] where the convolution of the cross sections, which depend of the energy of incident neutrinos, with thermal neutrino spectra was carried out; (ii) for the analysis of scattering of neutrinos with ^{12}C reanalyzing neutrino oscillations in the LSND experiment [7]; (iii) estimating events of supernova's neutrinos in ^{56}Fe using QRPA and projected QRPA (PQRPA) [18–21]; (iv) in the analysis of the influence of the configuration space for the scattering of ν_e with ^{12}C in the exclusive processes [22] (which take place from the ground state of the parent nucleus to the ground state of the daughter nucleus) and in the inclusive processes (when are included all transitions of the daughter nucleus); and (v) using the universality of weak interaction, the systematic in the calculation of muon capture rates was studied in nuclei with $A \leq 60$ [23].

We have used the original version of the GTBD [24] with some improvements introduced, such as a realistic description of the energy of the Gamow–Teller (GT) resonance peak [9]. In Ref. [9], the parameter σ_N associated with the width of the GT resonance was consistently adjusted to reproduce the β-decay and the EC rates for nuclei with $A \leq 70$. For this purpose, a careful selection of the most recent experimental data was performed, keeping only those values associated to allowed transitions (since the thermal fluxes used in current supernova simulations do not go beyond the 100 MeV of neutrino energy). After having fixed the parameters of the model, the reduced thermal cross section $\langle\sigma_\nu\rangle/A$ was estimated for all selected nuclei. From this study, we note that the results obtained for these cross sections within this global model are in accordance with the theoretical values obtained within more elaborated microscopic models, such as EFTSI + CQRPA from Ref. [17]. Thus, we can say that the GTBD is able to describe in a systematic way the nuclear properties of elements both in the β-stability line and in those exotic nuclei involved in the composition of presupernova in the region $A \leq 70$.

An extension of that work to nuclei with $A > 70$ would allow, due to the simplicity of the GTBD model, to study efficiently the region of neutron-rich nuclei where the r-process happens, as in the case of the neutrino wind. Neutrino–nucleus cross sections, $\sigma(E_\nu)$, are used to calculate neutrino capture rates competing with β-decay, as well as electron or positron captures, for example, in the r-process of nucleosynthesis. Several nuclear models are used to calculate these sections. When only allowed transitions are considered, $\sigma(E_\nu)$ can be written as a function of the number of protons of the target nucleus, Z, and the energy of the incident neutrino [8]. Our proposal consists of analyzing the $\sigma(E_\nu)$ obtained within the GTBD, and some particular cases using the QRPA and PQRPA models. Some specific sections will be compared with the expressions that appear in Bahcall's book [8] and others present in the literature. Let us try to obtain a new dependence as a function of

the atomic and mass numbers, Z and A, respectively, and observe deviations with respect to the E_ν^2 dependence for low energies. Disposing of such as polynomial expression for the cross sections can reduce computational time in calculations where many nuclei are taken into account, as for example, in the r-process of nucleosynthesis and in the calculation of the free-path medium for neutrinos in a supernova. We will select a set of nuclei for which the cross sections will be obtained within the GTBD models. Subsequently, we will proceed to adjust these sections to degree four polynomials as a function of neutrino energy. The coefficients of these adjustments will again be adjusted to a functional form, to be determined, depending on Z and A. Similar calculations were performed for the half-life of β-decay within the GTBD [25].

The paper is organized as follows. In Section 2, we present the main characteristics of the GTBD formalism. Still in this chapter, we deal with the cross-section $\sigma(E_\nu)$ which will be calculated using the GTDB. In Section 3, we show the results and discussions, and final conclusions are draw in Section 4.

2 Formalism

The evaluation of the ν_e-nucleus cross-section $\sigma(E_\nu)$ (which participates in the average cross section given in (1)) in a neutrino-rich environment, must be consistent with the procedure employed in calculating the β-decay rates (see Sect. 2 in Ref. [9]). The allowed transition approximation can be applied for relatively small momentum transfer (see Eq. (2.19) in Ref. [20]). Within this approximation, we have in natural units $\hbar = c = m_e = 1$ (n.u.):

$$\sigma(E_\nu) = \frac{G_F^2}{\pi}\int_0^{E_\nu - m_e} p_e E_e F(Z+1, E_e) \times \left[g_V^2 \left|\mathcal{M}_F(E)\right|^2 + g_A^2 \left|\mathcal{M}_{GT}(E)\right|^2\right] \mathrm{dE}. \quad (2)$$

Here, $G_F = (3.045647 \pm 0.0000002) \times 10^{-12}$ n.u. is the Fermi weak coupling constant, $g_V = g_A = 1$ are, respectively, the vector and axial-vector effective coupling constants, the argument of the matrix element, E, is the transition energy measured from the parent ground state, and E_e is the electron energy. Note that the true β-decay transition energy is $E_\beta = E_e + E_\nu = -E > 0$. The integration covers all possible nuclear states allowed by the selection rules, and the integration limits are determined from the energy conservation condition. When the energies are measured from the ground state of the parent nucleus (Z, A), this condition reads as follows:

$$E_\nu + M(Z, A) = E_e + M(Z+1, A) + Q_{\beta^-} + E, \quad (3)$$

where $E = E_\nu - E_e > 0$ is the excitation energy of the daughter nucleus $(Z+1, A)$, and $F(Z, E)$ is the usual scattering Fermi function which takes into account the Coulomb interaction between the electron and the nucleus. The Q_β value is the difference between neutral atomic masses of parent and daughter nuclei: $Q_{\beta^-} = M(A, Z) - M(A, Z+1) = B(A, Z+1) - B(A, Z) + m(nH)$ with $B(A, Z)$ and $B(A, Z+1)$ being the corresponding nuclear binding energies, and $m(nH) = m_n - m(^1H) = m_n - m_p - m_e = 0.782$ MeV. The masses were obtained in the same way as in [26]. This means that, when available, they are taken from the Wapstra–Audi–Hoekstra mass table [27] and, otherwise, they are determined from the Tachibana–Uno–Yamada semi-empirical mass formula [28].

The squares of the Fermi (F) and GT matrix elements are determined as follows:

$$\left|\mathcal{M}_X(E)\right|^2 = \int_{\epsilon_{\min}}^{\epsilon_{\max}} D_X(E, \epsilon) W(E, \epsilon) \frac{dN_1}{d\epsilon} d\epsilon, \quad (4)$$

for $X = F, \mathrm{GT}$. Here, $\epsilon_{\min}$ is the lowest single-particle energy of the parent nucleus and $\epsilon_{\max}$ is the energy of the highest occupied state. The one-particle-level density (proton or neutron), $\frac{dN_1}{d\epsilon}$, is determined by the Fermi gas model for the parent nucleus, and the weight function $W(E, \epsilon)$, constrained by $0 \le W(E, \epsilon) \le 1$, takes into account the Pauli blocking. Finally, $D_X(E, \epsilon)$, normalized as $\int_{-1}^{+1} D_X(E, \epsilon)\mathrm{dE} = 1$, is the probability that a nucleon with single-particle energy ϵ undergoes a β-transition. As in [24], we neglect the ϵ-dependence, i.e., it is assumed that all nucleons have the same decay probability, independent of their energies ϵ, $D_X(E, \epsilon) = D_X(E)$. For $D_X(E)$, we adopt a Gaussian-like distribution as follows [9]:

$$D_X(E) = \frac{1}{\sqrt{2\pi}\sigma_X} e^{-(E-E_X)^2/(2\sigma_X^2)}. \quad (5)$$

Here, E_X is the resonance energy, σ_X is the standard deviation, and the other quantities are defined as in [24]. When isospin is a good quantum number, the total Fermi strength $\int |\mathcal{M}_F(E)|\,\mathrm{dE} = N - Z$ is carried entirely by the isobaric analog state (IAS) in the daughter nucleus. However, because of the Coulomb force, the isospin is not a good quantum number and this leads to the energy splitting of the Fermi resonance. We will use the estimates introduced by Takahashi and Yamada [24], namely

$$E_F = \pm(1.44 Z_1 A^{-1/3} - 0.7825) \ \text{MeV, for } \beta^\pm \text{ decay},$$
$$\sigma_F = 0.157 Z_1 A^{-1/3} \ \text{MeV}, \quad (6)$$

where Z_1 is the proton number of the parent (daughter) nuclei for β^- (β^+ and EC) decay. The total GT strength in the (ν_e, e^-) channel is given by the Ikeda sum rule $\int |\mathcal{M}_{GT}(E)|\,\mathrm{dE} \simeq 3(N - Z)$, but its distribution cannot

be established by general arguments, and therefore must be either calculated or measured. Charge–exchange reactions (p, n) have demonstrated that most of the strength is accumulated in a broad resonance near the IAS [29–31]. In fact, even before these measurements were performed, Takahashi and Yamada [24] used the approximation as follows:

$$E_{\mathrm{GT}} \simeq E_F, \tag{7}$$

while σ_{GT} is expressed as follows:

$$\sigma_{\mathrm{GT}} = \sqrt{\sigma_F^2 + \sigma_N^2}, \tag{8}$$

with σ_N being the energy spread caused by the spin-dependent nuclear forces. For the Fermi transitions, we use the relation (6). Yet, for the GT resonance, instead of employing the approximation (7), we use the estimate as follows [24]:

$$E_{\mathrm{GT}} = E_F + \delta, \delta = 26A^{-1/3} - 18.5\frac{N-Z}{A}\ \mathrm{MeV}, \tag{9}$$

obtained by Nakayama et al. [32, 33] from the analytic fit of the (p, n) reaction data of nuclei near the stability line [29–31], where δ is positive. For the standard deviation σ_{GT}, we preserve the expression (8), and σ_N is treated as an adjustable parameter. All these quantities: σ_N, σ_X, and E_X, for $X = F$, GT, are expressed in units of MeV. Following Ref. [9], σ_N is determined through minimization of the function as follows:

$$\chi^2 = \sum_{n=1}^{N_0}\left[\frac{\log\left(\tau_{1/2}^{\mathrm{cal}}(n)/\tau_{1/2}^{\mathrm{exp}}(n)\right)}{\Delta\log\left(\tau_{1/2}^{\mathrm{exp}}(n)\right)}\right]^2, \tag{10}$$

where $\tau_{1/2}^{\mathrm{cal}}$ are the theoretical half-lives calculated within GTBD, N_0 is the number of experimental β-decay half-lives, $\tau_{1/2}^{\mathrm{exp}}$, selected fulfilling the conditions: (i) the branching ratio of the allowed transitions exceeds $\sim 50\%$ of the total β-decay branching ratio and (ii) the ground-state Q value is $\geq 10A^{-1/3}$ MeV, and

$$\Delta\log\left(\tau_{1/2}^{\mathrm{exp}}(n)\right) = \log\left[\tau_{1/2}^{\mathrm{exp}}(n) + \delta\tau_{1/2}^{\mathrm{exp}}(n)\right] - \log\left[\tau_{1/2}^{\mathrm{exp}}(n)\right], \tag{11}$$

and $\delta\tau_{1/2}^{\mathrm{exp}}(n)$ is the experimental error. This χ^2-function reinforces the contributions of data with small experimental errors. Moreover, we perform different fittings for even N-even Z $(e-e)$, odd N- odd Z $(o-o)$, odd N-even Z $(o-e)$, and even N-odd Z $(e-o)$ nuclei. Needless to say that, for $\tau_{1/2}^{\mathrm{exp}}$, we use here the most recent data [34], instead of those that were available when the GTBD was formulated [24]. The condition logft < 6 is imposed to include only the allowed β-decays.

3 Results and Discussions

The values of N_0 and the adjustable parameter σ_N at the minimal value of the χ^2-function are listed in Table 1 for the four different parity families of nuclei, for $\beta^{\pm}$ decay and EC. The σ_N values obtained minimizing the χ^2-function for the complete set of nuclei with $A < 220$ deviate from the underlined ones presented in Tables 1 and 2 from Ref. [9], adjusted only for the set of nuclei with $A \leq 70$, by no more than 10%. By this reason, we prefer to continue using the same values that in Ref. [9], which are shown in Table 1. Using these values for the adjustable parameter σ_N, we have calculated the theoretical values of the decay rates, $\tau_{1/2}^{\mathrm{cal}}$, for the complete set of 965 nuclei separated according to its parity. We show in Fig. 1 the results of $\log(\tau_{1/2}^{\mathrm{cal}}/\tau_{1/2}^{\mathrm{exp}})$ for β^- as a function of A in the heavy nuclei region $A < 220$. Similarly, in Fig. 2, we present the corresponding results for β^+ decay and EC. The results between the lines corresponding to the values -1 and 1 in those figures correspond to those nuclei in which the theoretical value differs from the experimental one in less than an order of magnitude. From these graphs, we can see that for those sets the model works well, since the experimental data are mostly close to the theoretical values. In fact, from Fig. 1, we see that the 72% of our calculated half-lives for the e–e group differ by less than one order of magnitude with the β^- data, 76% for the e–o set, 63% for the o–e one and 66% for the o–o set. Similarly, from Fig. 2, we see that the 52%, 60%, 55%, and 45% of our calculated half-lives for the e–e, e–o, o–e, and o–o nuclei, respectively, differ by less than one order of magnitude with the β^+ and EC data.

The ν_e-nucleus cross section evaluated consistently with the β-decay rates (see (2)) is shown in Figs. 3 and 4 for $\beta^{\pm}$ decay and EC process. These figures show the behavior of $\sigma(E_\nu)$ up to 250 MeV of incident neutrino energy. The multiple lines in these figures correspond to different values of A and Z. As previously discussed in Ref. [8], we clearly

Table 1 Number N_0 of nuclei with $A \leq 70$ used in the minimization process and σ_N standard deviations (in units of MeV) for $\beta^{\pm}$-decay and EC

N-Z (parent)	β^- decay		β^+ decay and EC	
	N_0	σ_N	N_0	σ_N
Even–even	139	15.8	149	9.9
Even–odd	187	16.5	198	12.2
Odd–even	175	7.2	204	11.8
Odd–odd	220	15.8	194	10.4

σ_N indicates the results obtained with E_{GT} approximated from (9)

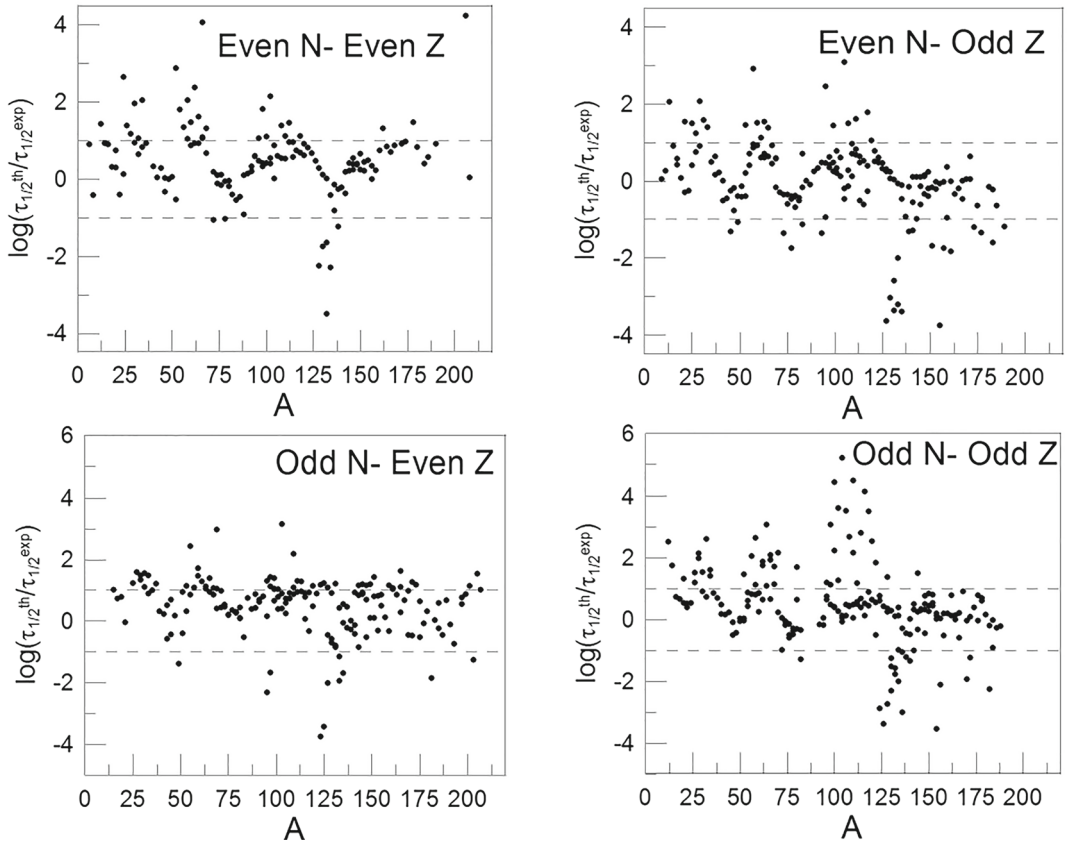

Fig. 1 $\log(\tau_{1/2}^{cal}/\tau_{1/2}^{exp})$ as a function of A for β^--decay of nuclei with $A < 220$

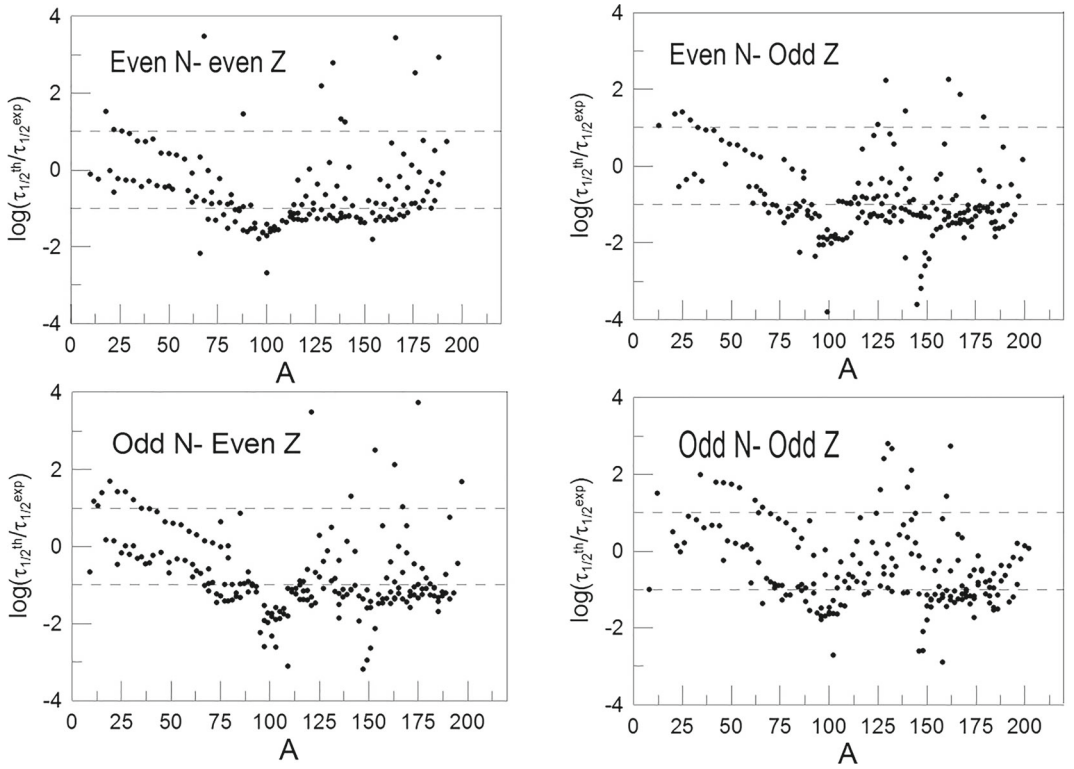

Fig. 2 $\log(\tau_{1/2}^{cal}/\tau_{1/2}^{exp})$ as a function of A for β^+-decay and EC of nuclei with $A < 220$

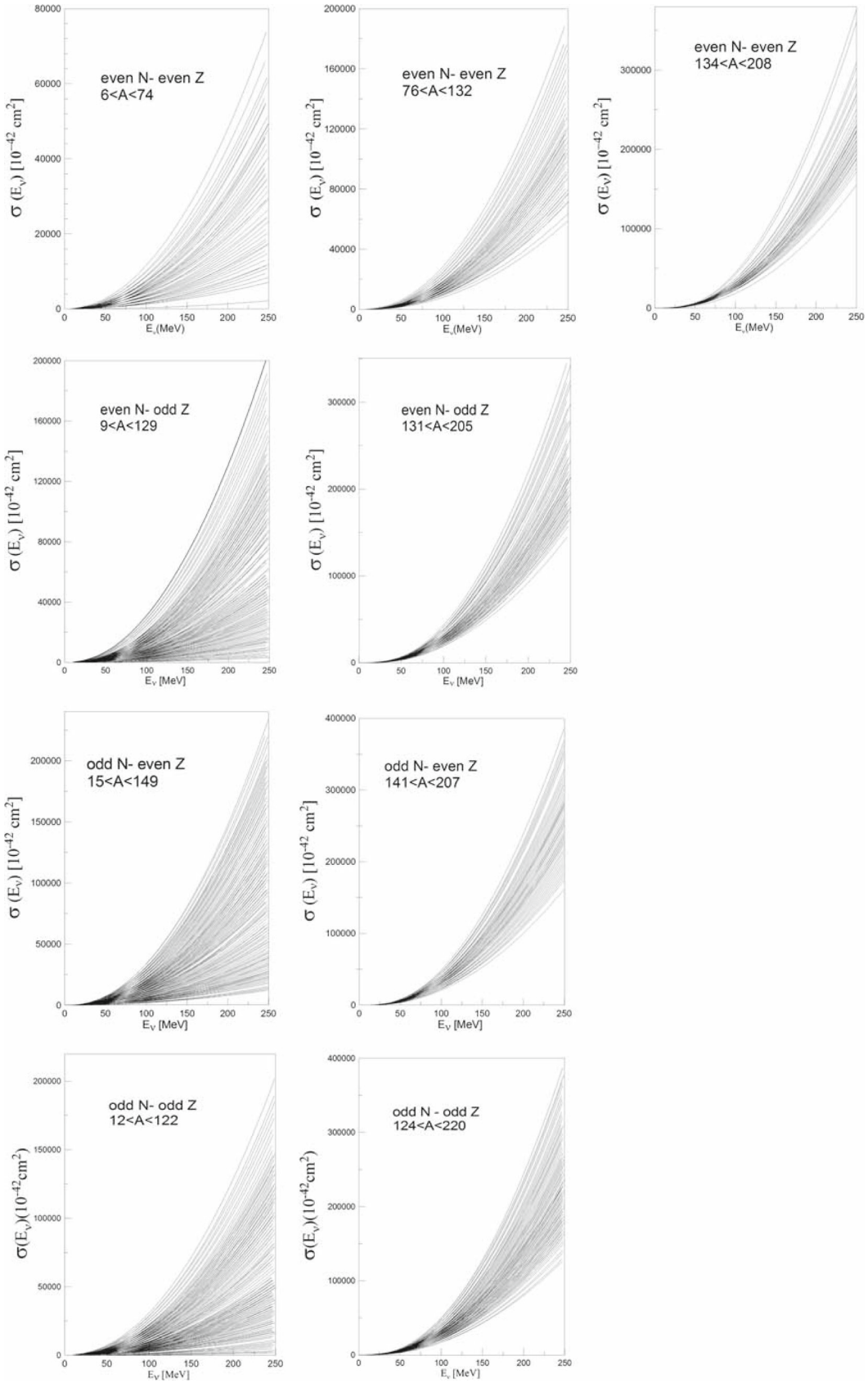

Fig. 3 Cross-section $\sigma(E_\nu)$ (in units of 10^{-42} cm^2) as a function of the neutrino energy (in units of MeV) for β^--decay. The multiple lines in these figures correspond to different values of A and Z

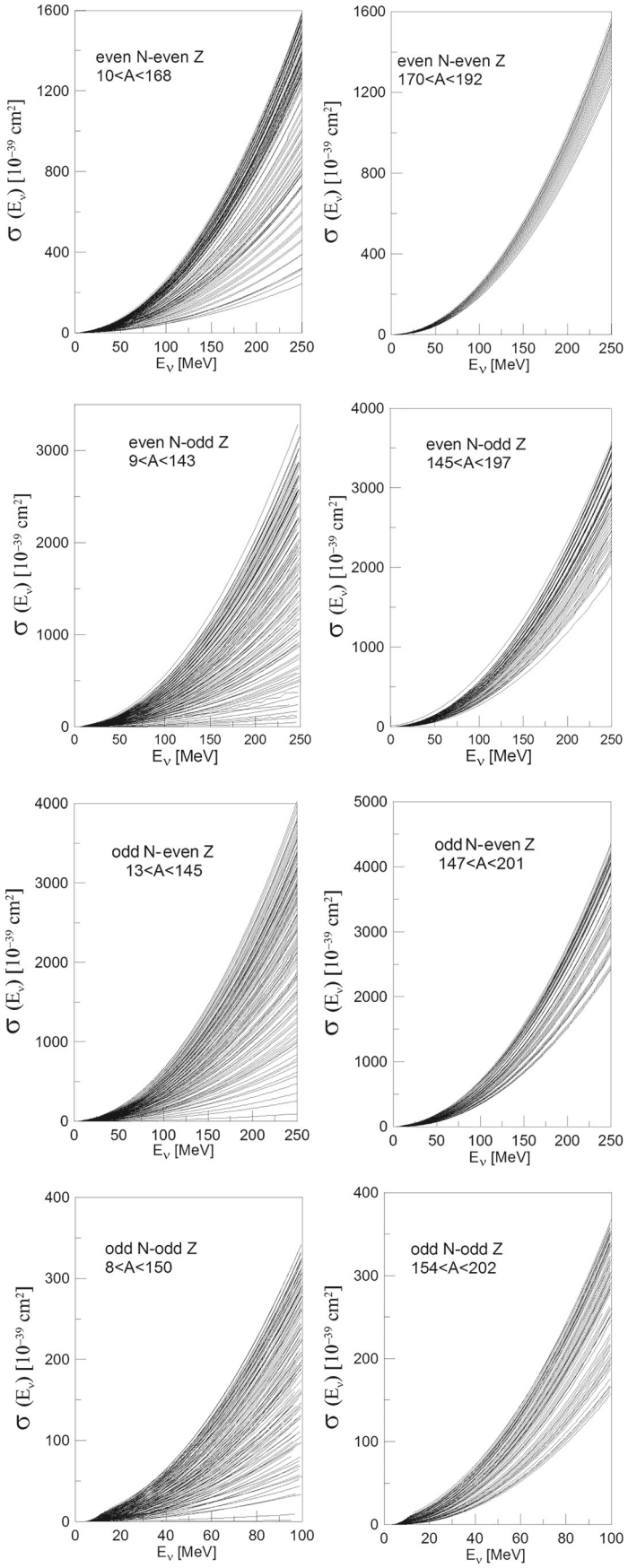

Fig. 4 Cross-section $\sigma(E_\nu)$ (in units of 10^{-39} cm^2) as a function of the neutrino energy (in units of MeV) for β^+-decay and EC. The multiple lines in these figures correspond to different values of A and Z

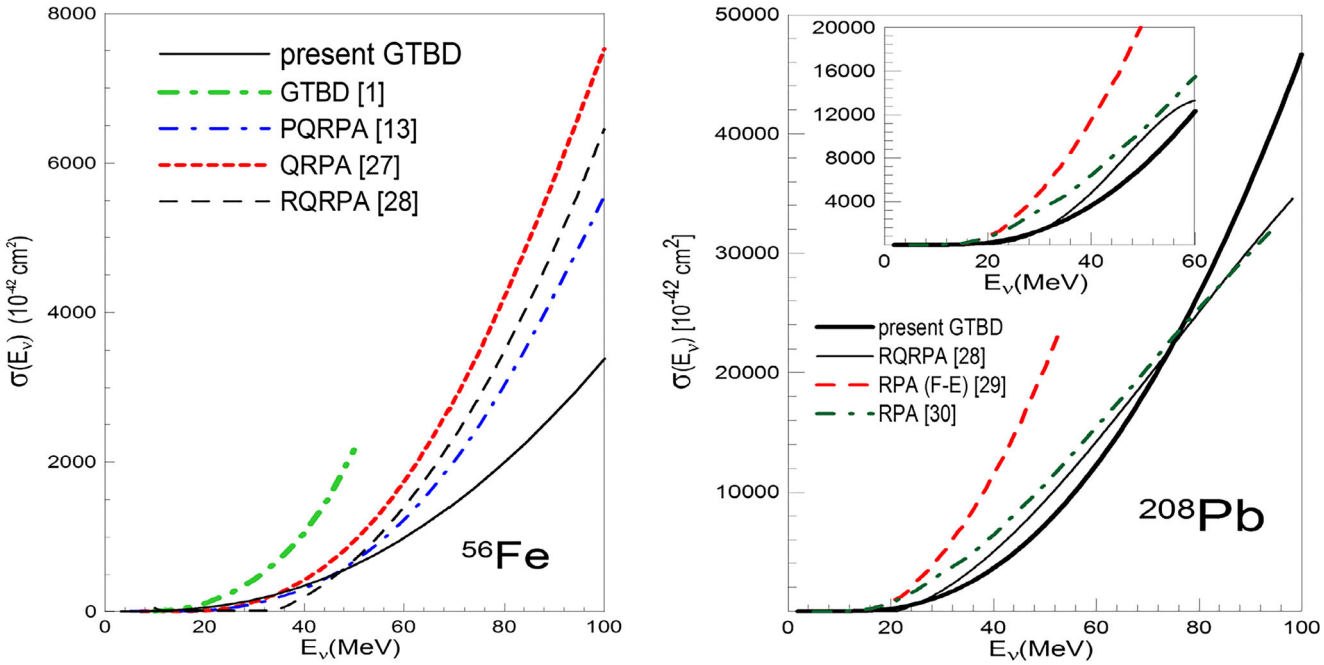

Fig. 5 Comparison of the neutrino–nucleus cross-section $\sigma(E_\nu)$ (in units of 10^{-42} cm^2) as a function of the neutrino energy (in units of MeV) for ^{56}Fe and ^{208}Pb within different models. See text for details

observe a growth with the neutrino energy of the quadratic type, that is, $\sigma(E_\nu) \sim E_\nu^2$, and also a growth with the value of mass number A.

We have compared our results obtained within the GTBD with those obtained using other more elaborate models. Indeed, in Fig. 5, we present the comparison of the cross sections for the electron neutrino–nucleus scattering process in the cases of ^{56}Fe and ^{208}Pb. There, we compare with the following models: (i) GTBD with other parametrization and including forbidden transitions [1, 2]; (ii) QRPA [35]; (iii) relativistic QRPA (RQRPA) [36]; (iv) PQRPA [18]; and (v) RPA obtained by interpolating between the Fermi function and the modified effective momentum approximation (RPA-(F-E)) [37, 38]. From Fig. 5, we observe that (a) for ^{56}Fe both GTBD approximations, the present one and that of Ref. [1, 2], are above the microscopic models up to an incident neutrino energy of $\sim$ 50 MeV; only the QRPA model presents a different result than the other microscopic models, a situation that will require a more detailed study in the future; (b) for ^{208}Pb, the GTBD calculation is below the microscopic models up to 70 MeV of energy of the incident neutrino. Another comparison with microscopic models can be made using the average cross section defined in (1). However, it is not our goal to calculate these averaged sections in the present work. A systematic calculation of them was carried out in Ref. [36] using the microscopic model RQRPA for even–even nuclei from oxygen to lead. As indicated above, the sections obtained within the microscopic models do not include all the degrees of freedom included in the GTBD. Therefore, we estimate that these $\langle\sigma_\nu\rangle_{\mathrm{RQRPA}}$ should show differences with our $\langle\sigma_\nu\rangle_{\mathrm{GTBD}}$, as in the example given previously for $\sigma(E_\nu)$ for ^{56}Fe and ^{208}Pb.

In order to obtain an expression that allows us to systematically calculate the neutrino–nucleus cross sections for a large group of nuclei, such as those usually needed in astrophysical calculations in presupernova stage, we propose a polynomial dependence of degree four in the incident neutrino energy for the cross section:

$$\sigma(E_\nu) = \sum_{i=0}^{4} A_i(A, Z) E_\nu^i. \tag{12}$$

We hope this expression to be an improvement compared to the proportionality to E_ν^2 mentioned in Ref. [8]. The coefficients $A_i(A, Z)$ are a function of the mass and atomic numbers, A and Z, respectively. As an example, we show in Fig. 6 these coefficients for the odd–odd group of nuclei decaying by β^-. We observe that the terms A_0 and A_2 grow with A and Z, while A_1 decreases. Also, the terms A_3 and A_4 decrease with A and Z, but being five to seven orders of magnitude smaller that the others. A similar behavior was observed for the coefficients for the other parity groups, both for $\beta^\pm$ decay and EC. Therefore, it makes sense to try to obtain a polynomial approximation of these coefficients $A_i(A, Z)$ as a function of A and Z, for each one of the eight sets we use. Kodama and Takahasi used such an expansion in Ref. [25] for the half-lives of beta decay and capture rates

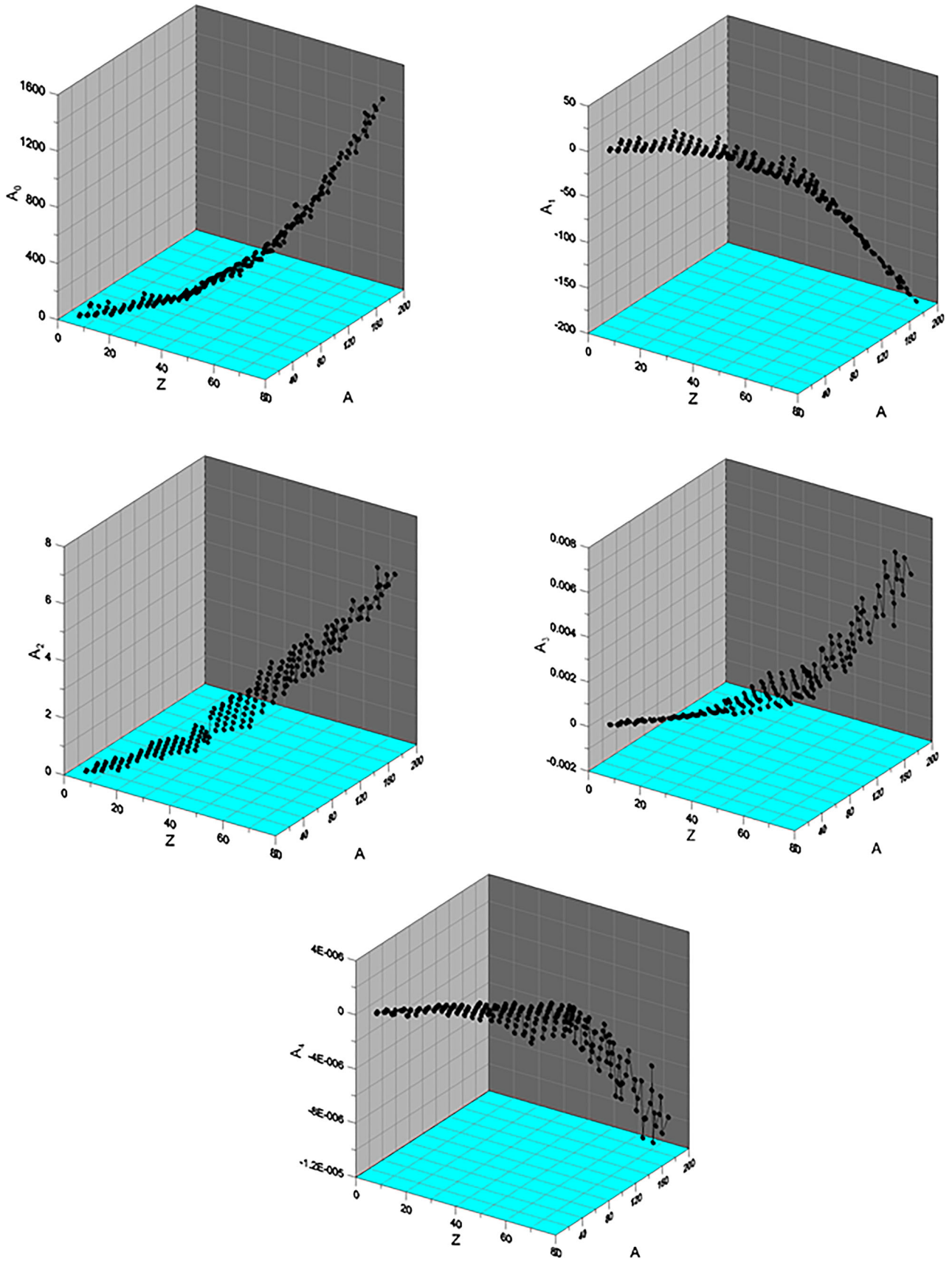

Fig. 6 Coefficients $A_i(A, Z)$ (in units of 10^{-42} cm^2/MeV^i) for odd–odd nuclei decaying by β^- emission

Table 2 Coefficients $d_{nm}^{(i)}$ (in units of 10^{-42} cm^2/MeV^i) for the odd–even set of nuclei decaying by β^-

i	0	1	2	3	4
$d_{01}^{(i)}$	7.1934	1.1045	2.6613×10^{-1}	-1.9562×10^{-1}	-1.5337×10^{-1}
$d_{02}^{(i)}$	-1.8493×10^{2}	1.2192×10^{1}	-8.9291×10^{-1}	6.8325×10^{-1}	3.4767×10^{-1}
$d_{11}^{(i)}$	-7.1896	9.98659×10^{-1}	-3.5646×10^{-2}	2.9960×10^{-2}	1.2479×10^{-2}
$d_{12}^{(i)}$	1.5819×10^{1}	-5.1828	1.2537×10^{-1}	-9.7811×10^{-2}	-1.5499×10^{-2}
$d_{21}^{(i)}$	2.0586×10^{-1}	-5.4498×10^{-1}	1.6877×10^{-3}	-1.1415×10^{-3}	-2.0892×10^{-4}
$d_{22}^{(i)}$	-2.4176×10^{-1}	2.4316×10^{-1}	-5.6416×10^{-3}	3.237×10^{-3}	-6.8046×10^{-4}
$d_{31}^{(i)}$	-1.6028×10^{-3}	9.0797×10^{-2}	-2.3653×10^{-5}	1.5254×10^{-5}	-9.6772×10^{-7}
$d_{32}^{(i)}$	-4.5427×10^{-3}	-3.78807×10^{-3}	6.1422×10^{-5}	-3.0764×10^{-5}	3.0722×10^{-5}
$d_{41}^{(i)}$	-4.3762×10^{-6}	-4.5341×10^{-6}	5.5783×10^{-8}	-5.9883×10^{-8}	2.4321×10^{-8}
$d_{42}^{(i)}$	9.3438×10^{-5}	1.7733×10^{-5}	1.0888×10^{-7}	8.8220×10^{-9}	-2.5739×10^{-7}

Table 3 Coefficients $d_{nm}^{(i)}$ (in units of 10^{-42} cm^2/MeV^i) for the even–odd set of nuclei decaying by β^-

i	0	1	2	3	4
$d_{01}^{(i)}$	-1.7545×10^{1}	-0.6950×10^{1}	-0.2953×10^{1}	-3.3867×10^{-2}	4.3911×10^{-1}
$d_{02}^{(i)}$	6.2798×10^{1}	1.4239×10^{1}	0.6853×10^{1}	-4.1965×10^{-1}	-0.1065×10^{1}
$d_{11}^{(i)}$	32.6134×10^{-1}	-1.5547×10^{-1}	1.2207×10^{-1}	-1.1295×10^{-2}	-2.4716×10^{-2}
$d_{12}^{(i)}$	-99.4070×10^{-1}	7.3306×10^{-1}	-1.5663×10^{-1}	9.1952×10^{-2}	4.1825×10^{-2}
$d_{21}^{(i)}$	-8.1073×10^{-2}	2.1472×10^{-3}	-1.6157×10^{-3}	5.5998×10^{-4}	3.3358×10^{-4}
$d_{22}^{(i)}$	2.2008×10^{-1}	8.9318×10^{-3}	-1.1190×10^{-3}	-3.7350×10^{-3}	3.8568×10^{-4}
$d_{31}^{(i)}$	9.5802×10^{-4}	6.0690×10^{-5}	1.0327×10^{-5}	-9.8016×10^{-6}	5.0512×10^{-7}
$d_{32}^{(i)}$	-2.7956×10^{-3}	-6.4131×10^{-4}	2.7297×10^{-5}	6.0277×10^{-5}	-2.4431×10^{-5}
$d_{41}^{(i)}$	-4.3256×10^{-6}	-7.6861×10^{-7}	-4.8613×10^{-8}	5.5492×10^{-8}	-2.2525×10^{-8}
$d_{42}^{(i)}$	1.4165×10^{-5}	5.5313×10^{-6}	4.2132×10^{-9}	-3.2689×10^{-7}	1.9788×10^{-7}

Table 4 Coefficients $d_{nm}^{(i)}$ (in units of 10^{-42} cm^2/MeV^i) for the even–even set of nuclei decaying by β^-

i	0	1	2	3	4
$d_{01}^{(i)}$	2.0672×10^{1}	3.1424	-8.4394×10^{-2}	-1.3943×10^{-1}	-1.1945×10^{-1}
$d_{02}^{(i)}$	-3.4471×10^{1}	-5.1573	2.2805×10^{-1}	-5.2186×10^{-1}	2.6770×10^{-1}
$d_{11}^{(i)}$	-4.3301×10^{-1}	-1.3765×10^{-1}	7.1454×10^{-3}	-5.0853×10^{-2}	6.3113×10^{-3}
$d_{12}^{(i)}$	-2.2975	-1.1347×10^{-1}	-8.4843×10^{-3}	2.7527×10^{-1}	-2.3949×10^{-3}
$d_{21}^{(i)}$	-2.5635×10^{-2}	8.0678×10^{-4}	6.0837×10^{-5}	2.5666×10^{-3}	-6.9838×10^{-5}
$d_{22}^{(i)}$	2.0375×10^{-1}	1.7911×10^{-2}	-9.5185×10^{-4}	-1.1007×10^{-2}	-6.4909×10^{-4}
$d_{31}^{(i)}$	5.238×10^{-4}	2.40278×10^{-5}	-2.0185×10^{-6}	-3.3749×10^{-5}	-1.4719×10^{-6}
$d_{32}^{(i)}$	-2.1393×10^{-3}	-3.7893×10^{-4}	1.5002×10^{-5}	1.0977×10^{-4}	2.2745×10^{-5}
$d_{41}^{(i)}$	8.7827×10^{-7}	-2.3612×10^{-7}	1.1042×10^{-8}	8.9829×10^{-8}	2.3857×10^{-8}
$d_{42}^{(i)}$	-1.7172×10^{-5}	2.2964×10^{-6}	-6.6630×10^{-8}	2.2563×10^{-8}	-2.0806×10^{-7}

Table 5 Coefficients $d_{nm}^{(i)}$ (in units of 10^{-42} cm^2/MeV^i) for the odd–odd set of nuclei decaying by β^-

i	0	1	2	3	4
$d_{01}^{(i)}$	4.7132×10^{1}	-5.5607	6.2888×10^{-2}	-9.8699×10^{-2}	-2.1587×10^{-1}
$d_{02}^{(i)}$	6.6852×10^{1}	1.9867×10^{1}	-2.0013×10^{-1}	3.5424×10^{-1}	5.9745×10^{-1}
$d_{11}^{(i)}$	3.3158×10^{-1}	1.4310	-3.6336×10^{-4}	1.8663×10^{-2}	2.4444×10^{-2}
$d_{12}^{(i)}$	7.3914	-4.2508	1.8127×10^{-2}	-6.3638×10^{-2}	-6.0399×10^{-2}
$d_{21}^{(i)}$	5.7069×10^{-2}	-6.1935×10^{-2}	4.7533×10^{-4}	-9.3344×10^{-4}	-8.6593×10^{-4}
$d_{22}^{(i)}$	-4.3740×10^{-1}	1.3463×10^{-1}	-3.1180×10^{-3}	3.0061×10^{-3}	1.6129×10^{-3}
$d_{31}^{(i)}$	-1.0313×10^{-3}	7.9729×10^{-4}	-1.7720×10^{-5}	1.7194×10^{-5}	1.1223×10^{-5}
$d_{32}^{(i)}$	6.2091×10^{-3}	-2.5550×10^{-4}	9.5345×10^{-5}	-5.0721×10^{-5}	-6.3774×10^{-6}
$d_{41}^{(i)}$	5.3930×10^{-6}	-1.9005×10^{-6}	1.3390×10^{-7}	-1.0662×10^{-7}	-4.0686×10^{-8}
$d_{42}^{(i)}$	-2.9579×10^{-5}	-1.7422×10^{-5}	-6.3824×10^{-7}	2.7754×10^{-7}	-1.2204×10^{-7}

Table 6 Coefficients $d_{nm}^{(i)}$ (in units of 10^{-39} cm^2/MeV^i) for the odd–even set of nuclei decaying by β^+ and EC

i	0	1	2	3	4
$d_{01}^{(i)}$	−2.5020	-2.5140×10^{-1}	6.7651×10^{-1}	−4.4468	-2.7059×10^{-1}
$d_{02}^{(i)}$	4.2320	4.2473×10^{-1}	-9.3563×10^{-1}	5.7657	-2.5728×10^{-1}
$d_{11}^{(i)}$	1.0481×10^{-1}	5.3570×10^{-3}	-2.9265×10^{-2}	1.6275×10^{-1}	1.1502×10^{-2}
$d_{12}^{(i)}$	1.0691×10^{-1}	2.3011×10^{-2}	-5.5515×10^{-2}	4.9517×10^{-1}	1.2883×10^{-1}
$d_{21}^{(i)}$	-3.3106×10^{-4}	1.2848×10^{-4}	-4.8998×10^{-5}	1.2229×10^{-3}	8.1307×10^{-4}
$d_{22}^{(i)}$	-1.5708×10^{-2}	-1.6728×10^{-3}	6.2967×10^{-3}	-4.5245×10^{-2}	-1.0745×10^{-2}
$d_{31}^{(i)}$	-2.6474×10^{-5}	-3.4646×10^{-6}	1.3377×10^{-5}	-1.0307×10^{-4}	-3.1766×10^{-5}
$d_{32}^{(i)}$	3.3961×10^{-4}	2.5941×10^{-5}	-1.4577×10^{-4}	1.0355×10^{-3}	2.5547×10^{-4}
$d_{41}^{(i)}$	2.4524×10^{-7}	2.0098×10^{-8}	-1.2589×10^{-7}	9.5328×10^{-7}	2.6306×10^{-7}
$d_{42}^{(i)}$	-2.1361×10^{-6}	-1.2499×10^{-7}	1.0090×10^{-6}	-7.3498×10^{-6}	-1.8076×10^{-6}

Table 7 Coefficients $d_{nm}^{(i)}$ (in units of 10^{-39} cm^2/MeV^i) for the even–odd set of nuclei decaying by β^+ and EC

i	0	1	2	3	4
$d_{01}^{(i)}$	1.3767	3.6476	2.6241	4.9956×10^{-1}	5.2905×10^{-1}
$d_{02}^{(i)}$	−2.3979	−6.5005	−4.6551	−3.8442	-5.3881×10^{-1}
$d_{11}^{(i)}$	-6.1000×10^{-2}	-2.1056×10^{-1}	-1.2487×10^{-1}	-1.1455×10^{-1}	-5.3331×10^{-3}
$d_{12}^{(i)}$	-2.6139×10^{-2}	1.1200×10^{-2}	-4.7679×10^{-2}	6.2206×10^{-1}	-1.1259×10^{-1}
$d_{21}^{(i)}$	5.9520×10^{-4}	2.1909×10^{-3}	9.7726×10^{-4}	4.9713×10^{-3}	-7.4539×10^{-4}
$d_{22}^{(i)}$	6.4347×10^{-3}	2.1805×10^{-2}	1.4826×10^{-2}	-2.5144×10^{-2}	7.1409×10^{-3}
$d_{31}^{(i)}$	7.1725×10^{-6}	3.4346×10^{-5}	2.3731×10^{-5}	-7.9085×10^{-5}	1.9192×10^{-5}
$d_{32}^{(i)}$	-1.5433×10^{-4}	-6.1210×10^{-4}	-3.7193×10^{-4}	3.8903×10^{-4}	-1.3285×10^{-4}
$d_{41}^{(i)}$	-1.0118×10^{-7}	-4.7733×10^{-7}	-2.8348×10^{-7}	4.3174×10^{-7}	-1.2931×10^{-7}
$d_{42}^{(i)}$	1.0585×10^{-6}	4.5406×10^{-6}	2.6197×10^{-6}	-2.0972×10^{-6}	7.9559×10^{-7}

Table 8 Coefficients $d_{nm}^{(i)}$ (in units of 10^{-39} cm^2/MeV^i) for the even–even set of nuclei decaying by β^+ and EC

i	0	1	2	3	4
$d_{01}^{(i)}$	2.8838	1.6427	1.6104	1.8038	1.6629
$d_{02}^{(i)}$	4.7557	−2.8714	−2.8723	−2.8527	−2.6823
$d_{11}^{(i)}$	1.1589×10^{-1}	-8.5894×10^{-2}	-7.8135×10^{-2}	-8.9227×10^{-2}	-8.5644×10^{-2}
$d_{12}^{(i)}$	1.2389×10^{-1}	-3.7724×10^{-3}	-7.1815×10^{-3}	-6.2733×10^{-2}	-4.4314×10^{-2}
$d_{21}^{(i)}$	-4.0612×10^{-4}	8.5373×10^{-4}	7.7885×10^{-4}	6.3748×10^{-4}	6.8888×10^{-4}
$d_{22}^{(i)}$	-1.6735×10^{-2}	8.3397×10^{-3}	7.3022×10^{-3}	1.2176×10^{-2}	1.0979×10^{-2}
$d_{31}^{(i)}$	-2.7001×10^{-5}	1.0791	8.5810×10^{-6}	2.0792×10^{-5}	1.8643×10^{-5}
$d_{32}^{(i)}$	3.5435×10^{-4}	-2.1181×10^{-4}	-1.8010×10^{-4}	-3.0514×10^{-4}	-2.8353×10^{-4}
$d_{41}^{(i)}$	2.5357×10^{-7}	-1.4494×10^{-7}	-1.1902×10^{-7}	-2.3645×10^{-7}	-2.2094×10^{-7}
$d_{42}^{(i)}$	-2.2206×10^{-6}	1.4466×10^{-6}	1.2136×10^{-6}	2.1447×10^{-6}	2.0201×10^{-6}

Table 9 Coefficients $d_{nm}^{(i)}$ (in units of 10^{-39} cm^2/MeV^i) for the odd–odd set of nuclei decaying by β^+ and EC

i	0	1	2	3	4
$d_{01}^{(i)}$	-3.1196×10^{-1}	1.9459	-3.2099×10^{-1}	-4.5446×10^{-1}	5.7636×10^{-1}
$d_{02}^{(i)}$	1.7499	−2.0284	5.4321×10^{-1}	7.9027×10^{-1}	−1.2834
$d_{21}^{(i)}$	3.0529×10^{-2}	-6.5969×10^{-2}	2.0838×10^{-2}	2.9783×10^{-2}	-3.2473×10^{-2}
$d_{12}^{(i)}$	-1.9419×10^{-1}	-2.9302×10^{-1}	7.9067×10^{-3}	1.1096×10^{-4}	3.7132×10^{-2}
$d_{21}^{(i)}$	-1.3532×10^{-3}	-1.1191×10^{-3}	-8.6955×10^{-5}	-2.3547×10^{-4}	6.7488×10^{-4}
$d_{22}^{(i)}$	8.7049×10^{-3}	2.3812×10^{-2}	-3.4884×10^{-3}	-3.9085×10^{-3}	5.2720×10^{-4}
$d_{31}^{(i)}$	2.5348×10^{-5}	5.3479×10^{-5}	-9.3705×10^{-6}	-9.4518×10^{-6}	-3.7210×10^{-6}
$d_{32}^{(i)}$	-1.5891×10^{-4}	-4.9837×10^{-4}	1.0289×10^{-4}	1.1890×10^{-4}	-3.7051×10^{-5}
$d_{41}^{(i)}$	-1.6052×10^{-7}	-4.2675×10^{-7}	1.0145×10^{-7}	1.1156×10^{-7}	-1.7893×10^{-8}
$d_{42}^{(i)}$	9.8059×10^{-7}	3.2122×10^{-6}	-7.8774×10^{-7}	-9.1394×10^{-7}	3.8888×10^{-7}

Table 10 Values of the rms_i (in units of 10^{-42} cm^2/MeV^i) for the set of nuclei decaying by β^-

	rms_0	rms_1	rms_2	rms_3	rms_4
Even-odd	1.46×10^2	4.92	5.59×10^{-1}	1.38×10^{-1}	1.27×10^{-1}
Odd–even	5.81×10^1	1.18×10^1	5.51×10^{-1}	7.39×10^{-2}	5.13×10^{-2}
Even–even	1.33×10^1	3.46×10^{-1}	9.51×10^{-2}	6.98×10^{-1}	4.51×10^{-2}
Odd–odd	1.48×10^1	4.85	2.90×10^{-1}	3.79×10^{-2}	3.58×10^{-2}

within the GTBD model. We propose the dependence as follows:

$$A_i(A, Z) = \sum_{m=1}^{4} \sum_{n=0}^{4} d_{nm}^{(i)} Z^n \alpha_m(A), \tag{13}$$

where the polynomial dependence with Z is implicit, while for the dependence with A, we include the terms $\alpha_1(A) = A$, $\alpha_2(A) = A^{2/3}$, $\alpha_3(A) = A^{-1/3}$, and $\alpha_4(A) = A^{-1}$. This dependence with the mass number A was inspired by the adjustment of coefficients in the liquid drop model, with a volumetric term proportional to A, a surface term proportional to $A^{2/3}$, a Coulombian term proportional to $A^{-1/3}$, and an asymmetry term proportional to A^{-1}. In order to reduce the number of free parameters and for simplicity, we decided not to use in this work the terms proportional to $A^{-1/3}$ and A^{-1}, that is,

$$\begin{aligned} A_i(A, Z) = &\left[d_{01}^{(i)} + d_{11}^{(i)} Z + d_{21}^{(i)} Z^2 + d_{31}^{(i)} Z^3 + d_{41}^{(i)} Z^4\right] A \\ &+ \left[d_{02}^{(i)} + d_{12}^{(i)} Z + d_{22}^{(i)} Z^2 + d_{32}^{(i)} Z^3 + d_{42}^{(i)} Z^4\right] \\ &\times A^{2/3}. \end{aligned} \tag{14}$$

Following the procedure used in Ref. [39] to fit the coefficients of the mass formula, the coefficients $d_{\text{mn}}^{(i)}$ will be determined by following the least squares method on the coefficients $A_i(A, Z)$. Naming $A_i^{\text{calc}}(A_j, Z_j)$ to the coefficient A_i calculated within the GTBD for the nuclear specie with atomic and mass numbers A_j and Z_j, respectively, this method select the coefficients $d_{\text{mn}}^{(i)}$ appearing in (14) that minimizes the "square error" function $\epsilon^2 = \sum_j \left[A_i(A_j, Z_j) - A_i^{\text{calc}}(A_j, Z_j)\right]^2$ and also gives the value of the root mean square (rms) deviation of the interpolation. This leads to the following set of ten linear equations with ten unknowns for each indexes $i = 0, \cdots, 4$, $n = 0, \cdots, 4$, $m = 1, 2$:

$$\begin{aligned} \frac{\partial \epsilon^2}{\partial d_{\text{nm}}^{(i)}} = &\, 2 \sum_{j=1}^{N_0} \left[A_i(A_j, Z_j) - A_i^{\text{calc}}(A_j, Z_j)\right] \\ &\times Z_j^n \alpha_m(A_j) = 0, \end{aligned} \tag{15}$$

which has exact solution. The rms will be calculated as follows:

$$\text{rms}_i = \sqrt{\frac{1}{N_0} \sum_{j=1}^{N_0} \left[A_i(A_j, Z_j) - A_i^{\text{calc}}(A_j, Z_j)\right]^2}. \tag{16}$$

The coefficients obtained with this method are given in Tables 2, 3, 4 and 5 for nuclei that decay by β^- and Tables 6, 7, 8 and 9 for nuclei that decay by β^+ and EC. For completeness, we present in Tables 10 and 11 the correspondent rms values. They are indicative of the confidence we can have in our results when we use the (12) and (14) to evaluate the neutrino–nucleus cross sections. Another way to quantify the fidelity of our results is to compare the graphs of $A_i^{\text{calc}}(A, Z)$ with the values of $A_i(A, Z)$ obtained from (14) using $d_{\text{nm}}^{(i)}$ from the Tables 2, 3, 4, 5, 6, 7, 8 and 9. For example, in Fig. 7, we present the graph of $A_i^{\text{calc}}(A, Z)$ and $A_i(A, Z)$ for the odd–odd set of nuclei that decay via β^-. There, we observe that only $A_0(A, Z)$ follows on average the values of $A_0^{\text{calc}}(A, Z)$ for all the nuclei within this set, while $A_1(A, Z)$, $A_2(A, Z)$, $A_3(A, Z)$ and $A_4(A, Z)$ show notable deviations in the last nuclei of the set ($A > 120$). Returning to Table 10 to look at the rms, we see that for $A_0(A, Z)$, we have an rms_0 of 14.8, which is the highest value for the rms of this set. The problem of deviations for values with $A > 120$ leads us to assume that it is necessary to include the other coefficients proportional to $\alpha_3(A) = A^{-1/3}$ and $\alpha_4(A) = A^{-1}$.

Table 11 Values of the rms_i (in units of 10^{-39} cm^2/MeV^i) for the set of nuclei decaying by β^+ and EC

	rms_0	rms_1	rms_2	rms_3	rms_4
Even–odd	3.29×10^{-1}	1.43×10^{-1}	1.12×10^{-1}	3.52×10^{-1}	3.51×10^{-1}
Odd–even	4.58×10^{-1}	2.21×10^{-1}	7.42×10^{-2}	1.00	1.91×10^{-1}
Even–even	3.29×10^{-1}	1.43×10^{-1}	1.12×10^{-1}	3.52×10^{-1}	3.51×10^{-1}
Odd–odd	7.08×10^{-1}	1.83×10^{-1}	5.76×10^{-2}	5.16×10^{-2}	5.16×10^{-2}

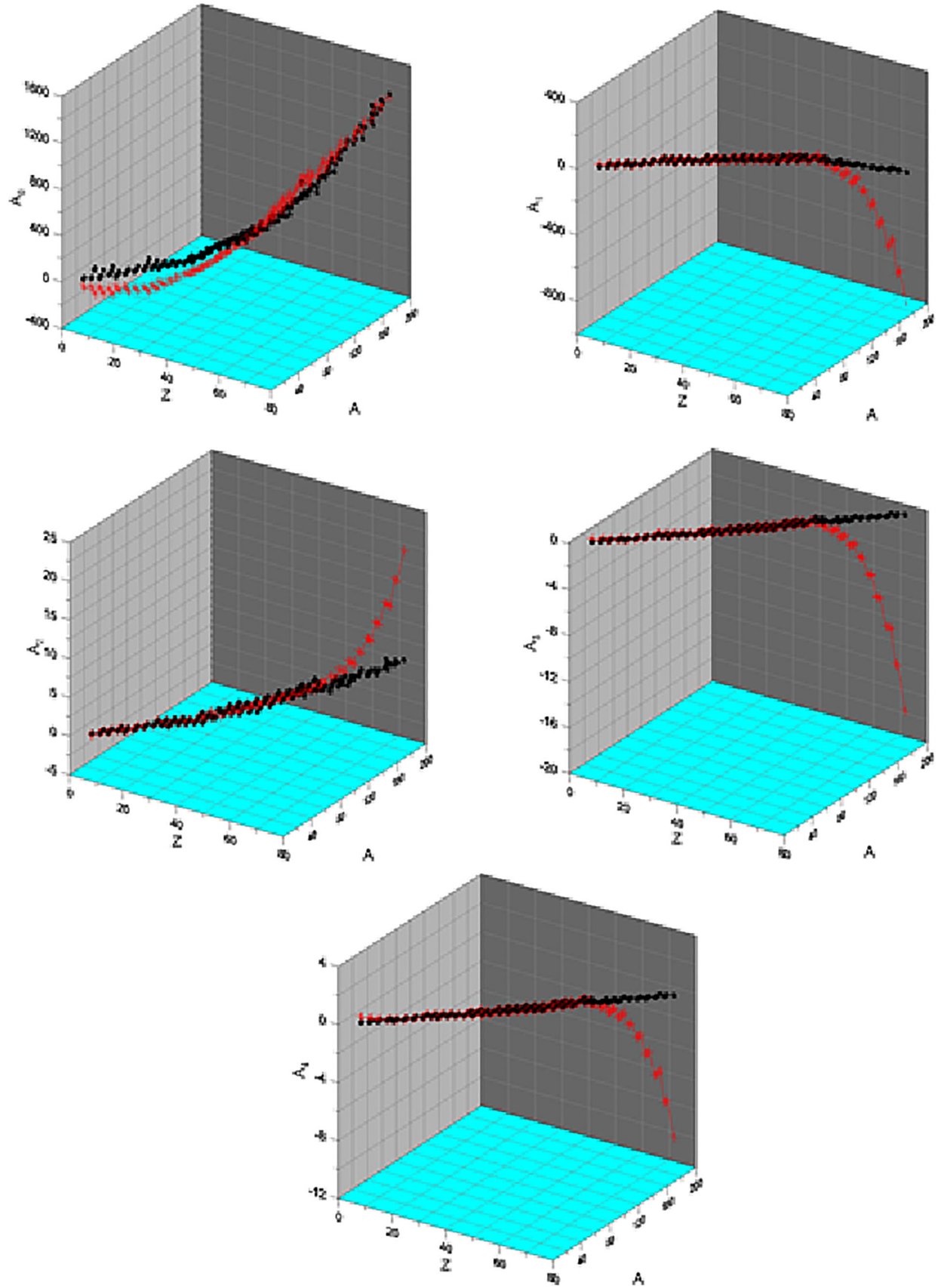

Fig. 7 Comparison of the coefficients $A_i^{\mathrm{calc}}(A, Z)$ and $A_i(A, Z)$ (in units of 10^{-42} cm^2/MeV^i) for odd–odd nuclei decaying by β^- emission

4 Concluding Remarks

We have studied the weak processes such as β-decay and electron capture within the standard elementary particle model using the GTBD nuclear model to describe the nuclei in the region $A < 220$ that participate in these reactions. Using the universality of weak interactions, where the same weak Hamiltonian can be used to describe the neutrino–nucleus scattering, we have calculated the neutrino–nucleus cross section for 965 nuclides. All these nuclei were separated into sets according to the mode of decomposition ($\beta^{\pm}$ and EC) and the parity of neutrons and protons ($e-e$, $e-o$, $o-e$, and $o-o$).

The experimental $\beta^{\pm}$ and EC decay rates that were used were selected by imposing the logft < 6 condition to include only allowed transitions in each set. As we have already mentioned, the processes $\beta^{\pm}$ and EC are fundamental in the scenario of stellar evolution (presupernova and supernova) and for nucleosynthesis (r-process). The decay rates mentioned compete, under certain stellar conditions, with neutrino capture rates and, for example, can modify the trajectory of the r-process. Neutrino capture rates are calculated with the neutrino–nucleus cross sections. The first estimates for these neutrino–nucleus cross sections were made by Bahcall who estimated that, at low energies of neutrinos incident, cross sections have a dependency proportional to E_{ν}^2. As we mentioned above, we have calculated these neutrino–nucleus cross sections using GTBD model that treats the nuclear matrix element obtained by the sum rule in parametric form, based on Fermi gas and including shell effects. For the single-particle distribution function, we used a Gaussian with a standard deviation that includes an adjustment factor σ_N, which comes from the propagation of energy caused by forces dependent on nuclear spin. For the parameter σ_N, we used the same values obtained in Ref. [9] for the set with $A < 70$, since we verified that the cross sections are only slightly modified when the parameter is varied by $\sim 10\%$. The neutrino–nucleus cross sections as a function of the incident neutrino energy, $\sigma(E_{\nu})$, obtained for $E_{\nu} < 250$ MeV, show in general a growth with the energy of the type E_{ν}^2, and also a growth with the mass number A. We also noticed that our results for cross sections show a good agreement with other previous evaluations within microscopic models such as QRPA [35], relativistic QRPA [36], projected QRPA [18], and RPA [37, 38] for ^{56}Fe and ^{208}Pb.

In order to improve the function that describes the behavior of the cross section as a function of neutrino energy, we have adjusted $\sigma(E_{\nu})$ to a four-degree polynomial in the incident neutrino energy through the formula (12). We have approximated the coefficients assuming a polynomial dependence with Z and a dependence with A, inspired by the adjustment of binding energies in the liquid drop model, with a volumetric term proportional to A, a surface term proportional to $A^{2/3}$, a coulombian term proportional to $A^{-1/3}$, and an asymmetry term proportional to A^{-1}. This fitting can be useful for those nuclei that are far from the β-stability line. The coefficients $d_{\mathrm{nm}}^{(i)}$ of (13) were determined using the method of minimum squares for each set of nuclei and for each process $\beta^{\pm}$ and EC, leading to the results shown in Tables 2, 3, 4, 5, 6, 7, 8 and 9. For simplicity, to reduce the number of free variables we have decided not to use the terms proportional to A^{-1} and $A^{-1/3}$ in this work. From the rms_i obtained (see Tables 10 and 11), we can say that in principle there is no correlation between every $A_i(A, Z)$ for each set. Another way to analyze the quality of our results was to compare the graphics of the $A_i^{\mathrm{calc}}(A, Z)$ with those of $A_i(A, Z)$ given by (14) with the $d_{\mathrm{nm}}^{(i)}$ obtained from our least squares method. We have observed that the deviations between both results are notorious for heavy nuclei. A possible improvement in these results could be obtained if terms proportional to A^{-1} and $A^{-1/3}$ were included. This will be a motivation for research in our future work. Additionally, we also plan to calculate the cross section averaged with the flows of thermal neutrinos to extend to the mass region $A < 220$ our results already discussed in [9] for $A < 70$.

Acknowledgments C.B. is fellow of the CONICET, CCT La Plata (Argentina). A.R.S. acknowledges the financial support of FAPESB (Fundação de Amparo à Pesquisa do Estado Bahia) TERMO DE OUTORGA PIE0013/2016. The authors thank the partial support of UESC (PROPP 00220.1300.1832).

References

1. N. Itoh, Y. Kohyama, A. Fujii, Nucl. Phys. A **287**, 501 (1997)
2. N. Itoh, Y. Kohyama, Nucl. Phys. A **306**, 527 (1978)
3. N.Yu. Agafonova et al., Astr. Phys., 27 (2007)
4. M. Antonello et al., [ICARUS Collaboration]. Eur. Phys. J. C **73**, 2599 (2013). https://doi.org/10.1140/epjc/s10052-013-2599-z, [arXiv:1307.4699 [hep-ex]]
5. R. Acciarri et al., [ArgoNeuT Collaboration]. Phys. Rev. D **95**(7), 072005 (2017). https://doi.org/10.1103/PhysRevD.95.072005 [arXiv:1610.04102 [hepex]]
6. K. Zuber, [HALO Collaboration]. Nucl. Part. Phys. Proc. **265–266**, 233–235 (2015). https://doi.org/10.1016/j.nuclphysbps.2015.06.059
7. A. Samana, F. Krmpotic, A. Mariano, R. Zukanovich Funchal, Phys. Lett. B **642**, 100 (2006)
8. J.N. Bahcall, *Neutrino Astrophysics* (Cambridge University Press, New York, 1989)
9. A.R. Samana, C.A. Barbero, S.B. Duarte, A.J. Dimarco, F. Krmpotic, New Jour. Phys. **10**, 033007 (2008)
10. C. Athanassopoulos et al., LSND Collaboration. Phys. Rev. C **54**, 2685 (1996)
11. C. Athanassopoulos et al., LSND Collaboration. Phys. Rev. Lett. **77**, 3082 (1996)
12. C. Athanassopoulus et al., LSND Collaboration. Phys. Rev. C **58**, 2489 (1998)

13. C. Athanassopoulus et al., LSND Collaboration. Phys. Rev. Lett. **81**, 1774 (1998)
14. A. Aguilar et al., LSND Collaboration. Phys. Rev. D **64**, 112007 (2001)
15. G.M. Fuller, B.S. Meyer, Astr. J. **453**, 792 (1995)
16. J.S. O'Connell, T.W. Donnelly, J.D. Walecka, Phys. Rev. C **6**, 719 (1972)
17. I.N. Borzov, S. Goriely, Phys. Rev. C **62**, 035501 (2000)
18. A.R. Samana, C.A. Bertulani, Phys. Rev. C **78**, 024312 (2008)
19. F. Krmpotic, A. Mariano, A. Samana, Phys. Lett. B **541**, 298 (2002)
20. F. Krmpotic, A. Samana, A. Mariano, Phys. Rev. C **71**, 044319 (2005)
21. A.R. Samana, F. Krmpotic, C.A. Bertulani, Comp. Phys. Comm. **181**, 1123 (2010)
22. A.R. Samana, F. Krmpotic, N. Paar, C.A. Bertulani, Phys. Rev. C **83**, 024303 (2011)
23. D. Sande Santos, A.R. Samana, A.J. Dimarco, F. Krmpotić, A systematic calculation of muon capture rates in the number projected QRPA. PoS XXXIVBWNP, 120. https://doi.org/10.22323/1.142.0120 (2011)
24. K. Takahashi, M. Yamada, Prog. Theor. Phys. **41**, 1470 (1969)
25. T. Kodama, K. Takahashi, Nuc. Phys. A **239**, 489 (1975)
26. T. Tachibana, M. Yamada, Y. Yoshida, Prog. Theor. Phys. **84**, 641 (1990)
27. A.H. Wapstra, G. Audi, R. Hoekstra, At. Data Nucl. Data Tables **39**, 281 (1988)
28. T. Tachibana, M. Uno, M. Yamada, S. Yamada, At. Data Nucl. Data Tables **39**, 251 (1988)
29. D.J. Horen et al., Phys. Lett. B **95**, 27 (1980)
30. D.J. Horen et al., Phys. Lett. B **99**, 383 (1981)
31. C. Gaarde et al., Nucl. Phys. A **369**, 258 (1981)
32. K. Nakayama, A.P. Galeao, F. Krmpotic, Phys. Lett. B **114**, 217 (1982)
33. K. Nakayama, A.P. Galeao, F. Krmpotic, Nucl. Phys. A **399**, 478 (1983)
34. B. Pritychenko, Nuclear Wallet Cards online at http://www.nndc.bnl.gov/wallet (2006)
35. R. Lazauskas, C. Volpe, Nucl. Phys. A **792**, 219 (2007)
36. N. Paar, D. Vretenar, T. Marketin, P. Ring, Phys. Rev. C **77**, 024608 (2008)
37. C. Volpe, N. Auerbach, C. Coló, N. Van Giai, Phys. Rev. C **65**, 044603 (2002)
38. J. Engel, G.C. McLaughlin, C. Volpe, Phys. Rev. C **67**, 013005 (2003)
39. C. Barbero, J.G. Hirsch, A. Mariano, Nucl. Phys. A **874**, 81 (2012)

Publisher's Note Springer Nature remains neutral with regard to jurisdictional claims in published maps and institutional affiliations.